

Research Paper

Cite this article: Liu Z, Chen X, Liu Q, Xie Z (2018). A blind signal detection algorithm for passive location system based on troposcatter. *International Journal of Microwave and Wireless Technologies* **10**, 1128–1133. <https://doi.org/10.1017/S1759078718001289>

Received: 6 March 2018

Revised: 14 August 2018

Accepted: 16 August 2018

First published online: 11 September 2018

Key words:

Complementary ensemble empirical mode decomposition; energy detection; entropy theory; passive location system; troposcatter

Author for correspondence:

Zan Liu, E-mail: kgdliuzan@163.com

A blind signal detection algorithm for passive location system based on troposcatter

Zan Liu, Xihong Chen, Qiang Liu and Zedong Xie

Air and Missile Defense College, Air Force Engineering University, Xi'an, 710051, Shaanxi, People's Republic of China

Abstract

To improve detection performance of passive location system based on troposcatter, we propose a blind signal detection algorithm. According to our algorithm, complementary ensemble empirical mode decomposition decomposes the received signal into several intrinsic mode functions (IMFs). To reconstruct the signal and background noises, difference between the entropy of adjacent IMFs is utilized as a standard. Different IMFs are utilized to estimate threshold of energy detection algorithm and energy level of received signal. Simulation examples indicate that the proposed algorithm can blindly and effectively detect the signal.

Introduction

Troposcatter which depends on scattering effect of low troposphere is a promising candidate for beyond line-of-sight (b-LoS) propagation. Electromagnetic (EM) wave of hostile radar propagated via troposcatter can be utilized for b-LoS location [1–3]. Priori knowledge of the signal received by a passive location system is probably absent [4]. EM wave propagated via troposcatter will also bear the deficiency of low signal to noise ratio (SNR) [5, 6]. Therefore, excellent signal detection algorithm is the prerequisite of passive location system based on troposcatter. Current signal detection mainly focuses on matched filter detection, cyclostationary feature detection, and energy detection (ED) [7–10]. Demand for priori knowledge of received signal contributes an evident drawback to matched filter detection. The huge calculation complexity of cyclostationary feature detection can bring a relatively long running time. Therefore, ED which has a simple implementation and needs little priori knowledge becomes a preferred candidate for passive location system.

Background noises varying with temperature and ambient interference can make the performance of ED get deteriorated [7]. The mobile position of passive location system and low SNR of signal will aggravate this drawback. Double-threshold ED has been proved an effective way to reduce the undesirable effect caused by varying noises. However, detection failure will occur as the energy level lies between two thresholds. Several researches have been committed to solve this problem. Cooperative signal detection (CSD) has been employed to overcome the possible failure [8]. Each terminal node sends two bit decision based on quantization when its observed energy lies within the confused region. Final decision about the presence or absence of a signal is made at fusion center (FC). A CSD based on weighted combination has also been proposed to improve the performance of double-threshold ED [9].

Most of above methods require the concrete knowledge of background noises. In [10], an adaptive signal detection has been proposed with noises variance estimation. Auto-regressive (AR) model is introduced to extract noises contained in the received signal. Similar to AR model, filtering models such as Kalman, wavelet transform can also effectively extract noises [11]. Nevertheless, several parameters of those models must be critically assigned, which severely requests for abundant experience of designers. Especially for the received signal without sufficient priori knowledge, this defect is more prominent. As a result, human intelligence plays a vital role in running those algorithms.

Considering absent priori knowledge and low SNR of signal received by a passive location system based on troposcatter, we propose a blind signal detection based on ED and an adaptive filtering model. The main innovation of this blind algorithm is that threshold of ED is acquired on the basis of background noises, which are extracted by an adaptive filtering model. Energy level of received signal is estimated according to the consequence of filtering model. The detection algorithm can enhance SNR and run without human intervention. As well, it does not depend on priori knowledge of received signal.

The rest of this paper is organized as follows. 'Passive location system based on troposcatter' section presents passive location system based on troposcatter. In 'Blind signal detection' section, a blind signal detection based on ED and an adaptive filtering model is introduced. In 'Example analysis' section, several examples are described to indicate the superiority of proposed signal detection. Finally, the conclusions are drawn in 'Conclusions' section.

Passive location system based on troposcatter

Figure 1 depicts passive location system based on troposcatter, which can effectively make a b-LoS detection and counter the anti-radiation missile. To obtain the location of enemy radar, it has at least three stations [12]. Distributed system has an inherent superiority at realizing CSD, which can effectively resist the undesirable shadow and multipath fading.

Only system makes a faultless decision, the next works will be carried out. In CSD, each node independently detects the signal and FC makes a global decision based on data fusion or decision fusion. The former consumes more wireless resources. On the other hand, performance of the latter could be improved remarkably by increasing the number of nodes [13].

As shown in Fig. 2, each terminal node of passive location system can be regarded as a FC. Local decision can be delivered by the reporting channel. According to decision fusion, u_i stands for the decision of node i , here $u_i = 1$ for the signal is present and $u_i = 0$ for the decision of absent signal. AND-rule and OR-rule can be adopted for decision fusion, the latter has a good performance and wide application [14]. According to OR-rule, FC can make global decision under an ideal condition as

$$\begin{cases} Q_{FA} = 1 - \prod_{i=1}^L (1 - P_{FA}), \\ Q_D = 1 - \prod_{i=1}^L (1 - P_D), \end{cases} \quad (1)$$

where Q_{FA} stands for the global probability of false alarm, Q_D the global probability of detection, L the number of terminal nodes, P_{FA} the terminal probability of false alarm, P_D the terminal probability of detection. Considering bit error rate (BER) of the reporting channel, we can obtain Q_{FA} and Q_D as

$$\begin{cases} Q_{FA} = 1 - \prod_{i=1}^L [(1 - P_{FA})(1 - P_e) + P_{FA}P_e], \\ Q_D = 1 - \prod_{i=1}^L [(1 - P_D)(1 - P_e) + P_DP_e], \end{cases} \quad (2)$$

where P_e refers to the BER. Detection problem can be transformed into a binary hypothesis test, thus

$$\begin{cases} H_0 : r[n] = w[n] & n = 0, 1, \dots, N - 1, \\ H_1 : r[n] = s[n] + w[n] & n = 0, 1, \dots, N - 1, \end{cases} \quad (3)$$

where H_0 refers to the absence of a signal, H_1 the presence of a signal, $s[n]$ the unknown deterministic signal, $w[n]$ the additive white Gauss noise (AWGN) with zero mean and σ^2 variance. According to ED [15], observed energy of signal can be expressed as

$$Y = \frac{1}{M} \sum_{n=1}^M |r(n)|^2, \quad (4)$$

where Y denotes the observed energy, M the number of samples taken under an observation period. If $Y > \tau$, $s[n]$ is present, otherwise the signal is absent. Here, τ stands for the predefined threshold. P_{FA} and P_D can be given as

$$\begin{cases} P_{FA} = \Pr(Y > \tau|H_0) = Q\left(\frac{\tau - \sigma^2}{\sigma^2 \sqrt{2/M}}\right), \\ P_D = \Pr(Y > \tau|H_1) = Q\left(\frac{\tau/\sigma^2 - (1 + \gamma)}{\sqrt{2/M}(1 + \gamma)}\right), \end{cases} \quad (5)$$

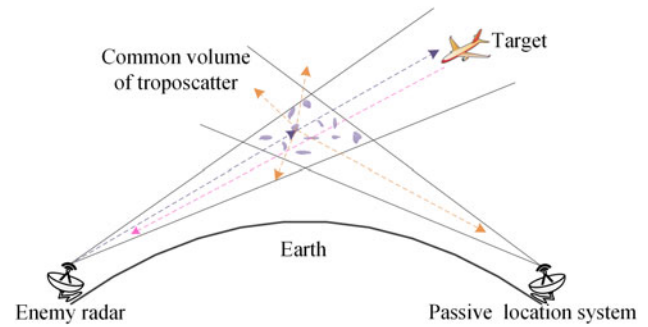


Fig. 1. Passive location system based on troposcatter.

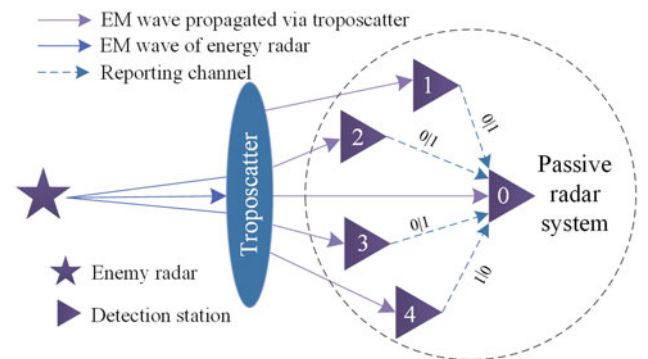


Fig. 2. Layout of CSD.

where γ denotes the SNR, $Q(\cdot)$ the Gaussian complement integral function, which can be given by

$$Q(x) = \frac{1}{\sqrt{2\pi}} \int_x^{+\infty} e^{-u^2/2} du. \quad (6)$$

Troposcatter can be approximated as a Rayleigh fading channel [16], we can acquire the probability distribution function of average SNR as

$$f(\gamma) = (1/\bar{\gamma})e^{-\gamma/\bar{\gamma}}, \quad (7)$$

where $\bar{\gamma}$ refers to the average SNR. Therefore, P_D can be given by

$$P_D = \int_0^{\infty} Q\left(\frac{\tau/\sigma^2 - (1 + \gamma)}{\sqrt{2/M}(1 + \gamma)}\right) f(\gamma) d\gamma. \quad (8)$$

An unstable environment can lead to varying noises. The uncertainty parameter of noises is uniformly distributed and can be expressed as

$$\rho = \frac{\sigma_u^2}{\sigma^2} \in [10^{-A/10}, 10^{A/10}], \quad A \geq 0. \quad (9)$$

Figure 3 shows the principle of double-threshold ED [8, 17], which is accepted as a viable solution to coping with the defect

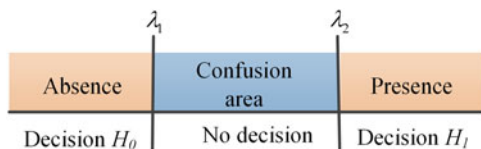


Fig. 3. Principle of double-threshold ED.

caused by varying noises. λ_1 and λ_2 denote two thresholds, which can be expressed as

$$\begin{cases} \lambda_1 = \left(\sqrt{\frac{2}{M} Q^{-1}(P_f) + 1} \right) \frac{1}{\rho} \sigma^2 \\ \lambda_2 = \left(\sqrt{\frac{2}{M} Q^{-1}(P_f) + 1} \right) \rho \sigma^2 \end{cases} \quad (10)$$

As equation (10), ρ and σ^2 need to be precisely estimated. A confusion area exists between λ_1 and λ_2 .

Figure 4 shows the P_D of CSD with the parameter $P_{FA} = 0.01$, $A = 0.5$, $\sigma^2 = 1$, $P_e = 10^{-4}$. It indicates that SNR has a great effect on signal detection. Meanwhile, large number of terminal nodes can lead to a better performance.

The main drawback of double-threshold ED is the confusion area and dependence on knowledge of background noises. Low SNR can contribute a poor performance to double-threshold ED. As known, troposcatter has a relatively high propagation loss and the received signal suffers from low SNR. Therefore, signal detection with good performance is in urgent need.

Blind signal detection

Filtering model

Empirical mode decomposition (EMD) based on Hilbert–Huang transform can decompose any complex signal into several sequences, which can be designated as intrinsic mode functions (IMFs). Every IMF represents a simple oscillatory mode [18]. Steps are as follows.

Steps of EMD
(1) Set $i = 1$, $r_0(t) = x(t)$.
(2) Identify all extremum of $r_{i-1}(t)$ and connect the sequential local maxima (minima) via cubic spline to drive $\max_{i-1}(t)$ ($\min_{i-1}(t)$), here $\max_{i-1}(t)$, $\min_{i-1}(t)$ denote the upper and lower envelopes, respectively.
(3) Define baseline $m_{i-1}(t)$ as the average of the upper and lower envelopes, namely $m_{i-1}(t) = [\max_{i-1}(t) + \min_{i-1}(t)]/2$.
(4) Extract local oscillation mode as $\text{IMF}_i(t) = r_{i-1}(t) - m_{i-1}(t)$. If mean $\text{IMF}_i(t)$ is 0, it can be treated as a true IMF, or else repeat steps (1)–(3) until its mean is 0.
(5) Compute the residue following $r_i(t) = r_{i-1}(t) - \text{IMF}_i(t)$.
(6) $i = i + 1$, return to step (2) until that the residue is a constant or the number of extremum is less than three.

The final consequences of EMD can be given by

$$x(t) = \sum_{i=1}^n h_i(t) + r_n(t), \quad (11)$$

where $x(t)$ denotes the original signal, $r_n(t)$ the remainder term, $h_i(t)$ the i th IMF. Each $h_i(t)$ has a single frequency. The first m

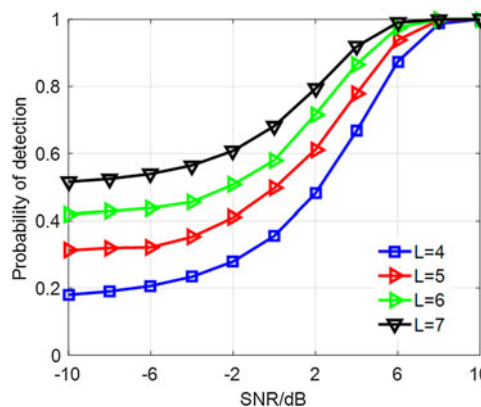


Fig. 4. P_D of CSD.

IMFs with high frequency are usually treated as background noises. The clean signal $f(t)$ and noises $s(t)$ can be reconstructed as

$$\begin{cases} f(t) = \sum_{i=m+1}^n h_i(t) + r_n(t), \\ s(t) = \sum_{i=1}^m h_i(t), \end{cases} \quad (12)$$

The primary weakness of EMD is mode mixing, which can be defined as a single IMF including oscillations of dramatically disparate scales, or a component of similar scale residing in different IMFs. When a signal is affected by interference, this problem is more likely to exist. Ensemble EMD (EEMD) can effectively copy with mode mixing [19]. According to EEMD, white noises are repeatedly added to the original data. Aim of above step is to homogenize signal scale in time-frequency space. As usual, variance of added white noise is $0.2\sigma_s^2$, here σ_s^2 is the variance of original data.

Figure 5 shows the process of EEMD, here, $\sqrt{N} = 0.2\sigma_s^2/e$. To regulate the precision and running time, value of e is usually assigned as 0.01. However, EEMD brings a new problem that the signal will be inevitably polluted by added white noises. Complementary EEMD (CEEMD) can reduce the reconstruction errors caused by the added white noises. According to CEEMD [20], white noises are added in pairs to the signal. The chief innovation of CEEMD can be expressed as

$$\begin{cases} r_{ij}^+(t) = f(t) + n_i(t), \\ r_{ij}^-(t) = f(t) - n_i(t). \end{cases} \quad (13)$$

Above noise-added data are decomposed via EMD. $c_{ij}^+(t)$ ($c_{ij}^-(t)$) represents the j th IMF derived from the i th noise-added data. The final IMF can be obtained as

$$\text{IMF}_j(t) = \frac{1}{N} \sum_{n=1}^N [c_{ij}^+(t) + c_{ij}^-(t)]. \quad (14)$$

As stated above, CEEMD can guarantee relatively actual IMFs. Then, the main problem is to determine parameter m in equation (12). To indicate uncertainty of determining m , we employ Heavysine signal added with different white noises as a reference. After decomposing signal on the basis of CEEMD, we successively reconstruct the signal and background noises according to equation (12). SNR is employed to evaluate the consequence, which is

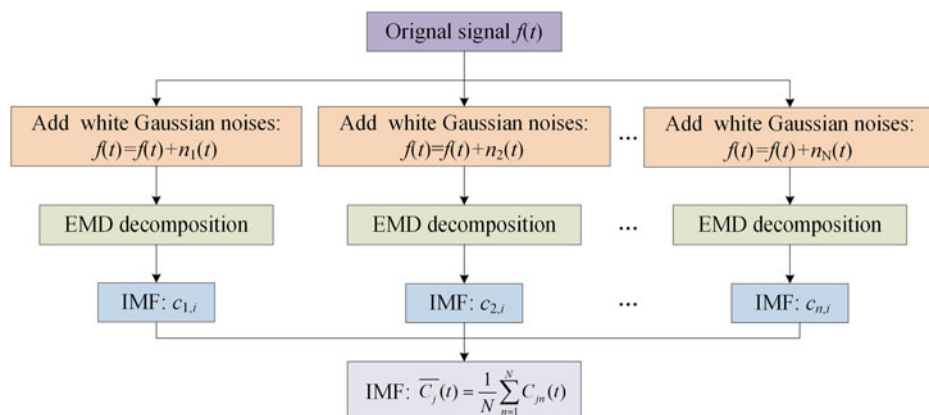


Fig. 5. Process of EEMD.

defined as

$$SNR = 10 \lg \left[\frac{\sum_{k=1}^M s_k^2}{\sum_{k=1}^M (s_k - g_k)^2} \right], \quad (15)$$

where s_k denotes the original Heavysine signal, g_k the reconstructed signal, M the sampling points. SNR with higher amplitude indicates that the reconstructed signal is more coincident with original signal. Namely, eliminated noises is more authentic.

Figure 6 displays SNR corresponding to different m . The respective characteristics of signals lead to different optimal m . Therefore, determining m is relatively difficult and needs abundant experiment. To accurately recognize IMFs, principal component analysis (PCA) is employed [21]. However, complex matrix operation existing in PCA may lead to a long running time. Entropy theory is accepted as an effective way to explicitly depict a signal, which can be expressed as [22]

$$H(x) = - \sum_{i=1}^L P(x = a_i) \log[P(x = a_i)], \quad (16)$$

where $P(x = a_i)$ stands for the probability of $x = a_i$. Entropy with a bigger value indicates that the signal is more unsteady and contains much more noises. The entropy of adjacent IMF is employed as a standard. Approach to determine m can be presented as follows.

Approach to determine m
(1) Decompose the received signal on the basis of CEEMD. (2) Calculate the entropy of each IMF. (3) Successively calculate the difference of adjacent entropy (ΔH). If β meets $\Delta H_{\beta+1} < \overline{\Delta H}$, then $m = \beta$.

Here

$$\overline{\Delta H} = \frac{1}{n-1} \sum_{i=1}^{n-1} \Delta H_i, \quad \Delta H_i = H_i - H_{i+1}. \quad (17)$$

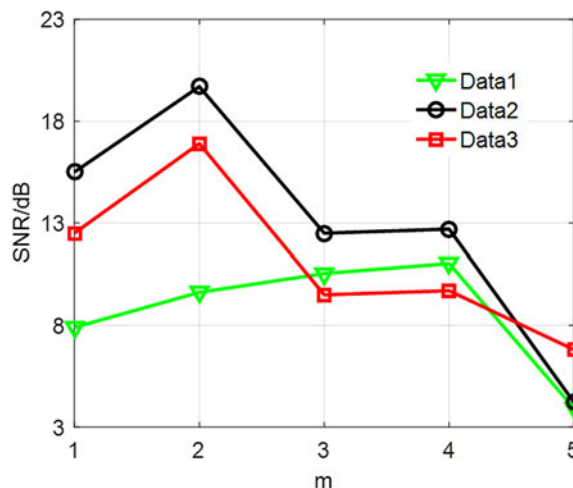


Fig. 6. SNR of proposed signals.

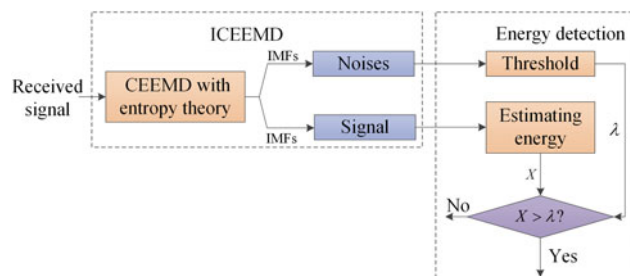


Fig. 7. Process of blind signal detection.

Signal detection based on ED and filtering model

Figure 7 shows the process of blind signal detection proposed in this paper. Firstly, CEEMD adaptively decomposes the signal received by passive system. Then, entropy theory described by equations (16) and (17) is used to precisely recognize consequences. IMFs treated as noises can be employed to calculate threshold of ED. Meanwhile, residual IMFs are used to estimate the observed energy on the basis of equation (4). In this way, SNR can be obviously enhanced. Because of CEEMD and entropy theory, the signal detection proposed in this paper can run

Table 1. SNR of original and processed signals.

Variance	Signals	A = 0.5	A = 1.0	A = 1.5
$\sigma^2 = 1.0$	Original signal	-4.09	-4.51	-4.65
	Wavelet model	-3.14	-3.51	-3.87
	AR model	-1.90	-2.32	-2.13
	ICEEMD model	-0.94	-1.22	-1.35
$\sigma^2 = 1.5$	Original signal	-5.94	-6.16	-6.55
	Wavelet model	-4.57	-5.53	-6.04
	AR model	-3.79	-4.07	-4.48
	ICEEMD model	-2.54	-2.72	-3.25

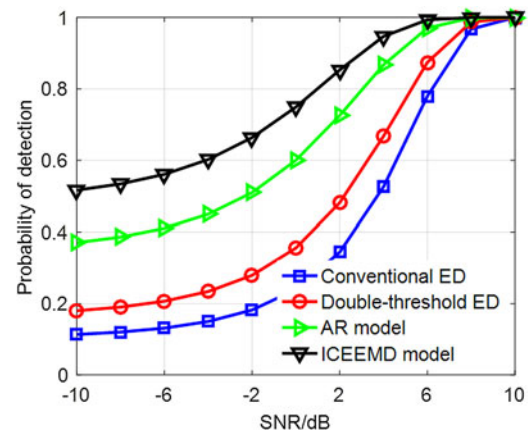


Fig. 9. SNR of signal processed by different models.

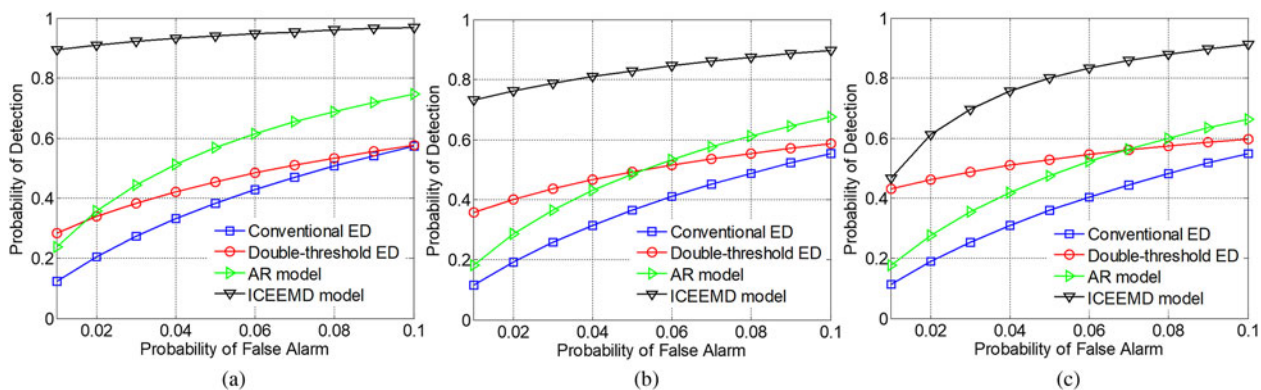


Fig. 8. ROC of energy detection improved by different models. (a) A = 0.5; (b) A = 1.0; (c) A = 1.5.

without human intervention, threshold can be constantly updated during the signal detection running. Because complicated matrix operations do not exist, its complexity can be approved.

To indicate the superiority of improved CEEMD (ICEEMD) model, a monopulse radar is treated as our target. Pulse wave added with AWGN is employed as received signal, amplitude and duty ratio of pulse wave is 2 and 5%, respectively. ICEEMD, wavelet, and AR models are employed to process the received signal. SNR described in equation (15) is also treated as a standard. Parameters of wavelet model have varied styles. After repeated simulations, model with db5 function, scale 5, and soft threshold function has the best performance among different wavelet models. Table 1 shows SNR of original signals and signals processed by different models. From Table 1, SNR is obviously enhanced by the filtering models to a certain extent. ICEEMD can most precisely reconstruct the signal. As well, AR model performs better than wavelet model.

Example analysis

In this section, above pulse wave with AWGN is also employed to imitate received signal. Figure 8 displays receiver operating characteristic of different ED with parameters: A = 0.5, $\sigma^2 = 1$, L = 4, $P_e = 10^{-4}$. Abscissa denotes the probability of false alarm; ordinate denotes the theoretical probability of detection. For conventional

ED, threshold is estimated according to the background noises extracted by ICEEMD; original received signal is employed to estimate the energy level. For double-threshold ED, A and σ^2 are available. ICEEMD model denotes the blind signal detection proposed in this paper. Because AR model performs better than wavelet model, we employ it as a reference. Similar to ICEEMD model, background noises and observed energy are estimated by the AR model. Figure 9 shows theoretical P_D changing with SNR with the same parameters and $P_{FA} = 0.01$. Abscissa denotes the SNR of received signal.

As shown in Fig. 8, ICEEMD model can better improve ED than AR model. Although double-threshold ED can somewhat improve the performance of signal detection, knowledge of background noises must be available.

Figure 9 also indicates the superiority of the blind signal detection algorithm proposed in this paper. Because ICEEMD and AR models can enhance the SNR, these two models have better performance with the low SNR than conventional models. During above simulations, the blind signal detection can run without priori knowledge and user intervention.

Conclusions

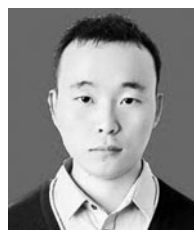
In this work, considering the absent knowledge and low SNR of received signal, we propose a blind signal detection algorithm to

improve the detection performance of passive location system based on troposcatter. CEEMD improved by entropy theory is proposed to process the received signal, and ED is operated on the basis of consequences. This model can run without human intervention and effectively copy with the varying noises. Simulation examples indicate that the blind signal detection proposed in this paper can effectively detect the signal. It can also be employed for the cognitive radio system.

Acknowledgements. The authors declare that there is no conflict of interests regarding the publication of this paper. This work was supported by the National Natural Science Foundation of China under grant No. 61671468 and 61701525. It also was supported by Postdoctoral Science Foundation of China under grant No. 2017M623351.

References

1. Wang Z, Wang M, Wang Q, Cheng Z and Zhang X (2017) Receiving antenna mode of troposcatter passive ranging based on the signal group delay. *IET Microwaves, Antennas & Propagation* **11**, 121–128.
2. Wang M, Wang Z, Wang J and Cheng Z (2017) Fading correlation modelling for troposcatter microwave propagation in array antenna detection applications. *IET Microwaves, Antennas & Propagation* **11**, 833–843.
3. Wang Q, Wang Z, Cheng Z and Wang M (2014) The troposcatter array signal receiving model and processing algorithm. *12th International Conference on Signal Processing (ICSP)*, Hangzhou, China, pp. 283–287.
4. Yang F, Xu Q and Li B (2017) Ship detection from optical satellite image based on saliency segmentation and structure-LBP feature. *IEEE Geoscience & Remote Sensing Letters* **14**, 1–5.
5. Dinc E and Akan OB (2015) A ray-based channel modeling approach for MIMO troposcatter beyond-line-of-sight (b-LoS) communications. *IEEE Transactions on Communications* **63**, 1690–1699.
6. Luini L, Riva C, Emiliani L and Capsoni C (2016) Worst-month tropospheric attenuation prediction: application of a new approach. *European Conference on Antennas & Propagation*, Davos, Switzerland, pp. 1–5.
7. Bae S, So J and Kim H (2017) On optimal cooperative sensing with energy detection in cognitive radio. *Sensors* **17**, 1–15.
8. Verma P and Singh B (2016) Overcoming sensing failure problem in double threshold based cooperative spectrum sensing. *Optik* **127**, 4200–4204.
9. Liu X, Zhang C and Tan X (2014) Double-threshold cooperative detection for cognitive radio based on weighing. *Wireless Communications and Mobile Computing* **14**, 1231–1243.
10. Joshi DR, Popescu DC and Dobre OA (2010) Adaptive spectrum sensing with noise variance estimation for dynamic cognitive radio systems. *44th Annual Conference on Information Sciences and Systems*, Princeton, USA, pp. 1–5.
11. Song X, Zhou C, Hepburn DM and Zhang G (2017) Second generation wavelet transform for data denoising in PD measurement. *IEEE Transactions on Dielectrics & Electrical Insulation* **14**, 1531–1537.
12. Zhuang M and Wang Z (2017) Troposcatter array signal detection based on frequency and spatial fading correlation. *Electronics Letters* **53**, 1564–1566.
13. de Paula A and Panazio C (2014) Cooperative spectrum sensing under unreliable reporting channels. *Wireless Networks* **20**, 1399–1407.
14. Yue W, Zheng B, Meng Q, Cui J and Xie P (2011) Robust cooperative spectrum sensing schemes for fading channels in cognitive radio networks. *Science China (Information Sciences)* **54**, 348–359.
15. Chatziantoniou E, Allen B, Velisavljevic V, Karadimas P and Coon J (2017) Energy detection based spectrum sensing over two-wave with diffuse power fading channels. *IEEE Transactions on Vehicular Technology* **66**, 868–874.
16. Li C, Chen X and Liu X (2018) Cognitive tropospheric scatter communication. *IEEE Transactions on Vehicular Technology* **67**, 1482–1491.
17. Ahuja B and Kaur G (2017) Design of an improved spectrum sensing technique using dynamic double threshold for cognitive radio networks. *Wireless Personal Communications* **3**, 1–24.
18. Li J, Wang J, Zhang X and Tang W (2017). Empirical mode decomposition based on instantaneous frequency boundary. *Electronics Letters* **53**, 781–783.
19. Liu Z, Cui Y and Li W (2017) A classification method for complex power quality disturbances using EEMD and rank wavelet SVM. *IEEE Transactions on Smart Grid* **6**, 1678–1685.
20. Xu Y, Luo M, Li T and Song G (2017) ECG signal de-noising and baseline wander correction based on CEEMDAN and wavelet threshold. *Sensors* **17**, 1–16.
21. Sharifi R and Langari R (2017) Nonlinear sensor fault diagnosis using mixture of probabilistic PCA models. *Mechanical Systems & Signal Processing* **85**, 511–521.
22. Lim M and Yuen PC (2016) Entropy measurement for biometric verification systems. *IEEE Transaction on Cybernetics* **46**, 1065–1077.



Zan Liu received the B.S. and M.S. degrees in 2013 and 2015, respectively, from Air Force Engineering University, Xi'an. He is currently working toward the Ph.D. degree in the Air and Missile Defense College. His research interests include information theory and passive radar system.



Xihong Chen received the M.S. degree in communication engineering from Xidian University, Xi'an, in 1992 and the Ph.D. degree from Missile College of Air Force Engineering University in 2010. He is currently a professor with Air and Missile Defense College, AFEU, Xi'an. His research interests include information theory, information security, and signal processing.



Qiang Liu received the B.S. and M.S. degrees in 2017 and 2009, respectively, from Air Force Engineering University, Xi'an. He has got his Ph.D. degree in 2013, also from the Air Force Engineering University. His research interests include information security and signal processing.



Zedong Xie received the B.S. and M.S. degrees in 2012 and 2014, respectively, from Air Force Engineering University, Xi'an. He is currently working toward the Ph.D. degree in the Air and Missile Defense College. His research interests include MIMO-OFDM in troposcatter communications and anti-jamming techniques.